THEORY OF TRACTION OF A WHEEL MOVING ON THIN VISCOUS MUD FILM

Thesis for the Degree of M. S. MICHIGAN STATE UNIVERSITY Bong-Sing Chang 1965 THESIS

LIBRARY Michigan State University

THEORY OF TRACTION OF A WHEEL MOVING ON THIN VISCOUS MUD FILM

bу

BONG-SING CHANG

A THESIS

Submitted to
THE COLLEGES OF AGRICULTURE AND ENGINEERING
of Michigan State University
in partial fulfillment of the requirements
for the degree of

MASTER OF SCIENCE

Department of Agricultural Engineering

1965

ABSTRACT

THEORY OF TRACTION OF A WHEEL MOVING ON A VISCOUS MUD FILM

by Bong-sing Chang

A supersaturated viscous oil overlaying a hard, plane ground is often critical to locomotion in many areas due to the lubricating effect of the thin layer of viscous mud.

In the theoretical analysis of this problem, equations for the total lift force and the friction force of a wheel moving on a thin layer viscous mud were obtained. In order to illustrate the equations, a simplified numerical example was described.

A Ring-disk Viscometer was developed to measure the viscosity of the mud. Soil was packed in the viscometer and allowed to dry. After water was added a rotating steel disk was pressed against the soil. Strain gages were used for the torque and axial force transducers, which indicated the shear stress and normal pressure. The result of the measurement showed that the shear stress increases linearly when the normal pressure increases. A considerable influence on the shear stress

Bong-sing Chang

from the velocity was also found. This means that for a given load, a vehicle can obtain a greater pull when its slip speed is increased.

Approved

Major Professor

Approved

Department Chairman

ACKNOWLEDGEMENT

The author wishes to express his sincere thanks to Dr. Sverker Persson for his continual suggestions and guidance during the investigation.

Sincere appreciation is extended to Dr. T. H. Wu of the Department of Civil Engineering and Prof. H. F. McColly of the Department of Agricultural Engineering for serving on the Guidance Committee and for their helpful suggestions.

The author feels deeply indebted to Dr. A. W. Farrall, former chairman of Agricultural Engineering Department and Dr. C. W. Hall, chairman of Agricultural Engineering Department for granting the graduate research assistantship that made this thesis possible.

Partial support has also been received from the.

U. S. Army, Detroit Procurement District which is also deeply appreciated.

The efforts and assistance of Mr. James Cawood and Mr. Glenn Shiffer are sincerely appreciated.

Special credit must be given to Mr. and Mrs.

Nung-shing Chang, the author's parents and Mr. and Mrs.

Jain-Li Kao, the author's best friends for their encouragement and financial support that helped to complete this work.

The author wishes to express his deepest sorrow

to Mrs. Chei-Quen Chen for her husband was dead in an air crash in Taiwan in 1964. Mr. and Mrs. Chen encourage and support me to come to the United States to fulfill my advanced study.

May, 1965

TABLE OF CONTENTS

		Fage
PART	1: THEORETICAL ANALYSIS	
1.	Introduction	2
2.	Literature review on the lubrication theory-	5
3.	Some basic assumptions	33
4.	Characteristics of the velocities	10
5.	The velocity function	14
6.	The general precoure equation	16
7.	The lift and friction forces equations	18
೮.	A calculation example	22
	•	
PART	II: EXPERIMENTAL WORK	
	(The viscosity of the mud film)	
9.	Review of literature on viccommuters	20 f
10.	The Cone Viscometer and the Ring-disk Viscometer	33
11.	Procedures of operating the Ring-dick Viscometer	3 7
12.	Results, discussions and conclusion	40

REFERENCES

LIST OF FIGURES

TITOT	Or.	r 10 UKBS	Гаде
Fig.	1;	Tapered bearing moving over the lubricant film	6
Fig.	2;	The deformation of the wheel in the thin layer of viscous mud	Ģ
Fig.	3;	Analysis and transformation of the velocities	11
Fig.	4 ;	The element of the fluid	14
Fig.	5;	The forces on the element	14
Fig.	6;	The assumed contact zone	17
Fig.	7;	The forces on any point of the surface of the wheel	e 13
Fig.	8;	The Deformation of a wheel on the mud film is a r-y coordinate system	20
Fig.	9;	Simplified diagram of Fig. 8 for calculation example	22
Fig.	10;	The coaxial-cylinder type viscometer	27
Fig.	11;	The cone-plate type viscometer	29
Fig.	12;	The disk type viscometer	29
Fig.	13;	The cone-cylindrical type viscometers	30
Fig.	L4;	The Cone Viscometer	31
Fig.	15;	The Ring-disk Viscometer	32
Fig.	16;	The design principle of the Vis- cometers	35
Fig.	17;	The total view of the Ring-disk Viscometer and its recording systems	3 5
Fig.	18;	Soil sample of the Ring-disk Visco-meter before testing	35
Fig.	L9;	During testing (Ring-disk Viscometer)	36
Fig.2	20;	Soil sample after testing (Ring-disk Viscometer)	3 6

LIST OF	FIGURES : Continued.	Page
Fig.21;	The lubrication grooves on the Ring-disk Viscometer	39 39
Fig.22;	a. Normal Pressure (σ) vs. Shear Stress (γ) (soil condition 1)	41
	b. Enlarged portion of Fig. 22a	4 2
Fig.23;	a. Hormal Pressure (σ) vs. Shear stress (γ) (soll condition 2)	4 3
	b. Enlarged portion of Fig. 23a	4 1
Fig.24;	Film thickness (\S) vs. normal pressure (σ)(soil condition 2)	47
Fig.25;	Film thickness (\S) vs. normal pressure (σ) (Soil condition 1)	4 5

FART I

THEORETICAL ANALYSIS

I. Introduction

A supersaturated viscous soil overlaying a hard, plane ground is often critical to locomotion in many areas. The purpose of this thesis is to evaluate the pressure and friction force under a wheel moving across a relatively thin viscous mud overlaying a rigid, flat bottom. A similar case is the journal bearing which is supported by a loadcarrying thin film of lubrication oil laying between the journal and the bearing cell. The thin layer of viscous mud could be considered as the lubricating film between a moving wheel and the rigid ground.

Many similar examples are available for this problem—such as the vehicles moving on the wet high—way, airplanes landing and taking off on a wet airstrip, or vehicles crossing over field composed of a over—saturated viscous mud overlaying a hard bottom.

In the theoretical treatment of this studying only two-dimensional flow is considered. The actual three-dimensional flow will be considered in a more advanced stage of study of this problem. Therefore, it is only a very fundamental study of the traction of vehicles in the viscous mud area.

Previous work which relates to this problem is limited. The studies found are listed below.

T. Czako and E. Hegedus (1958) considered the motion resistance in extremely loose soils on the basis of fluid dynamics since such soils behave like viscous fluids rather than granular masses. The viscosity resistance caused by fluid is called friction drag ($\rm D_f$). Another type of drag, $\rm D_p$, is produced by the dynamic pressure $\rm PV^2/2$ acting on the normal projected area of a body perpendicular to the flow lines. Thus

$$D_{\mathbf{f}} = C_{\mathbf{f}} \rho \frac{\mathbf{v}^2}{2} A_1$$

$$D_{\mathbf{p}} = C_{\mathbf{p}} \rho \frac{\mathbf{v}^2}{2} A_2$$

There;

f: density of the fluid

V : velocity

 $^{\rm A}$ l : normal projected area perpendicular to the flow lines

A2: wetted area

 $\mathbf{C}_{\mathbf{f}}$: friction drag coefficient

 C_n : pressure drag coefficient

The total drag D_{\pm} is sum of the above equations

$$D_{t} = C_{d} \int \frac{v^{2}}{2} A_{2}$$

Where;

$$c_d = c_f \frac{A_1}{A_2} + c_p$$

Czako and Hegedus showed that the drag coefficient

($C_{\rm d}$) depends on a constant value C and Reynolds number $R_{\rm n}$

$$C_d = \frac{C}{R_n} = \frac{C \gamma}{V d}$$

where;

V : velocity

d : depth of the immersed body

y: kinematic viscosity (ratio of dynamic viscosity to density.)

Tests performed with wheels in loose mud indicate the usefulness of viscosity and density notions in an evaluation of motion resistance.

Tests were made by E. Hogedus (1958) for evaluating of the drag resistance on different shapes (rectangular, tire shape, parabolic) of wheel by the Viscous Soil Drag Test Apparatus. Strain gage recording was used. Test results showed that the rectangular shape wheel obtained highest drag and the parabolic shape wheel obtained the lowest drag.

2. Review of Literature on the Lubrication Theory

Dubrication and viscosity, which are interconnected, play a most vital role in our great and complex civilization. Viscosity is defined as the physical property of a fluid which offers resistance to relative motion of its parts. It corresponds to an internal fluid friction produced by the molecules of the lubricant as they flow past one another. The greater this relative motion, the greater is the internal resistance that the lubricant offers.

The earliest theory of viscosity was published in 1668 by Sir Isaac Newton (1642-1727) on the viscous, or laminar, flow. Newton asserted that there is a property of a fluid that resembles friction between two solid surfaces. "Two concentric cylinders which were submerged in deep and quiet water" was his basic experiment. He observed that a force was required to cause relative rotational motion of one cylinder with respect to the other. The force required was

$$P = KA - \frac{V}{h}$$

where;

R: coefficient of viscosity or what we new know as absolute viscosity μ .

A : area

V: relative velocity of the two cylinders.

h: distance between the two surfaces or the thickness of the water film.

In lubrication analysis we assume that the velocity in the flow is a continuous function of the film thickness. In above equation we could replace V/h by dV/dh to get the more general relationship.

$$x' = \mathcal{M} A \frac{dV}{dh}$$

In stress form

$$\gamma = \mu \frac{dV}{dh}$$

These equations give the same result for the case considered by Newton.

By the application of above theory, a hydrodynamic theory was developed for the general bearing problems. One of the bearing problems we are interested in is that of a tapered plane bearing moving relatively over a stationary base (Fig. 1) and separated from it by a thin lubricant film

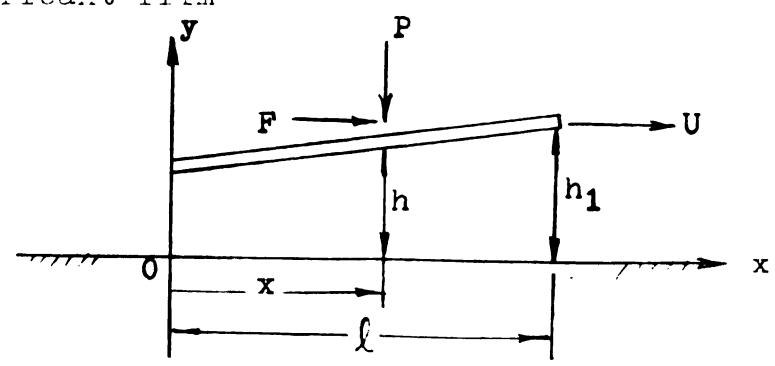


Fig. 1; Tapered bearing maving or or the lubricant film.

In this case, it has been found (Fuller, 1956) that the total lifting force to the bearing is

$$\mathbf{P} = \frac{6\mu \mathbf{U} \mathbf{k}}{2} \mathbf{k}_{\mathbf{p}} \mathbf{b}$$

where;

$$k_{p} = \frac{1}{m!} \left[\frac{m' + 1}{-(2 + m')(1 + m'x/\ell)} + \frac{1}{(1 + m'x/\ell)} - \frac{1}{2 - m'} \right]$$

$$m' = \frac{h_1}{h_2} - 1$$

U: velocity of the bearing

The total friction force on the bearing is

$$F = \mu b \int \frac{u}{h_2} k_f$$

where;

$$k_{f} = \frac{4}{m!} \log_{e} (1+m!) - \frac{6}{2+m!}$$

b= width of the element

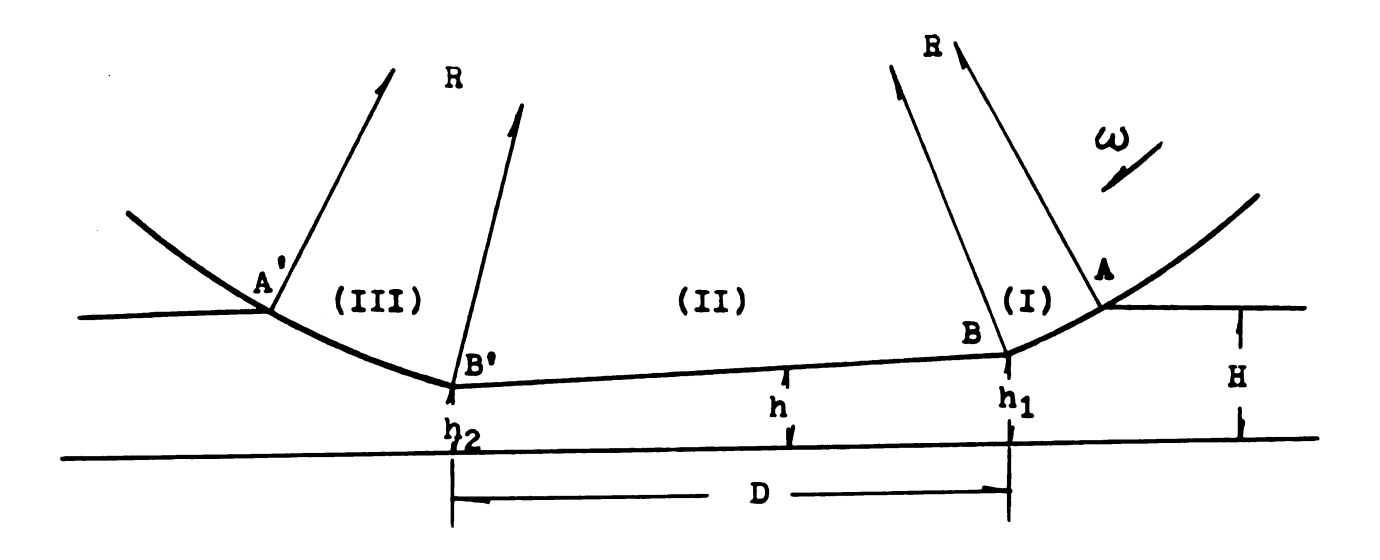
3. Some Basic Assumptions.

Some basic assumptions must be made in order to limit the difficulties of this problem.

- a), The wheel has a smooth surface.
- b), The wheel is in a cylindrical shape. (not circular)
- c), The viscous mud (a clay suspension) acts as a Newtonian fluid.
- d), The thickness of the viscous soil film is relatively small and it is overlaying a rigid, flat ground.
- e), The ground is assumed rigid, therefore, the deflection of the ground by applying a weight (wheel) can be neglected.
- f), The assumed deformed shape of the wheel (a rubber tire with an air pressure pa) in the viscous film is shown by Fig. 2.

Before the theoretical analysis being made, the following important assumptions also should be stated.

- a), This problem is analyzed as a two-dimensional flow.
- b), The pressure in the viscous soil film under the state of Fig. 2 is a variable only in x-direction. It means the pressure in ydirection remains a constant. The reason is that the thickness of the film compared to the other dimensions is small.
- c), The velocity in the film is a function of both x and y directions.
- d), The viscosity of the mud suspension as it is being passed through by the wheel remains constant.
- e), The viscous mud is incompressible.



- R: radius of wheel
- ω: angular velocity of the wheel
- U: velocity of the vehicle
- H: thickness of the viscous soil film before passage of the wheel
- D: deformation distance of the wheel bottom
- h; thickness of the film under point B
- h_2 : thickness of the film under point B^{\bullet}
- h: thickness of the film under any point

Fig. 2. The deformation of the wheel in the thin layer of viscous mud.

4. Characteristics of velocities;

There are two velocities present in this problem, namely U and ω . U is the forward velocity of the wheel center, ω is the angular velocity of the wheel. Therefore, the linear velocity of any point on the wheel surface is $V=R\omega$ which is relative to the wheel center, where R is the radius of the wheel.

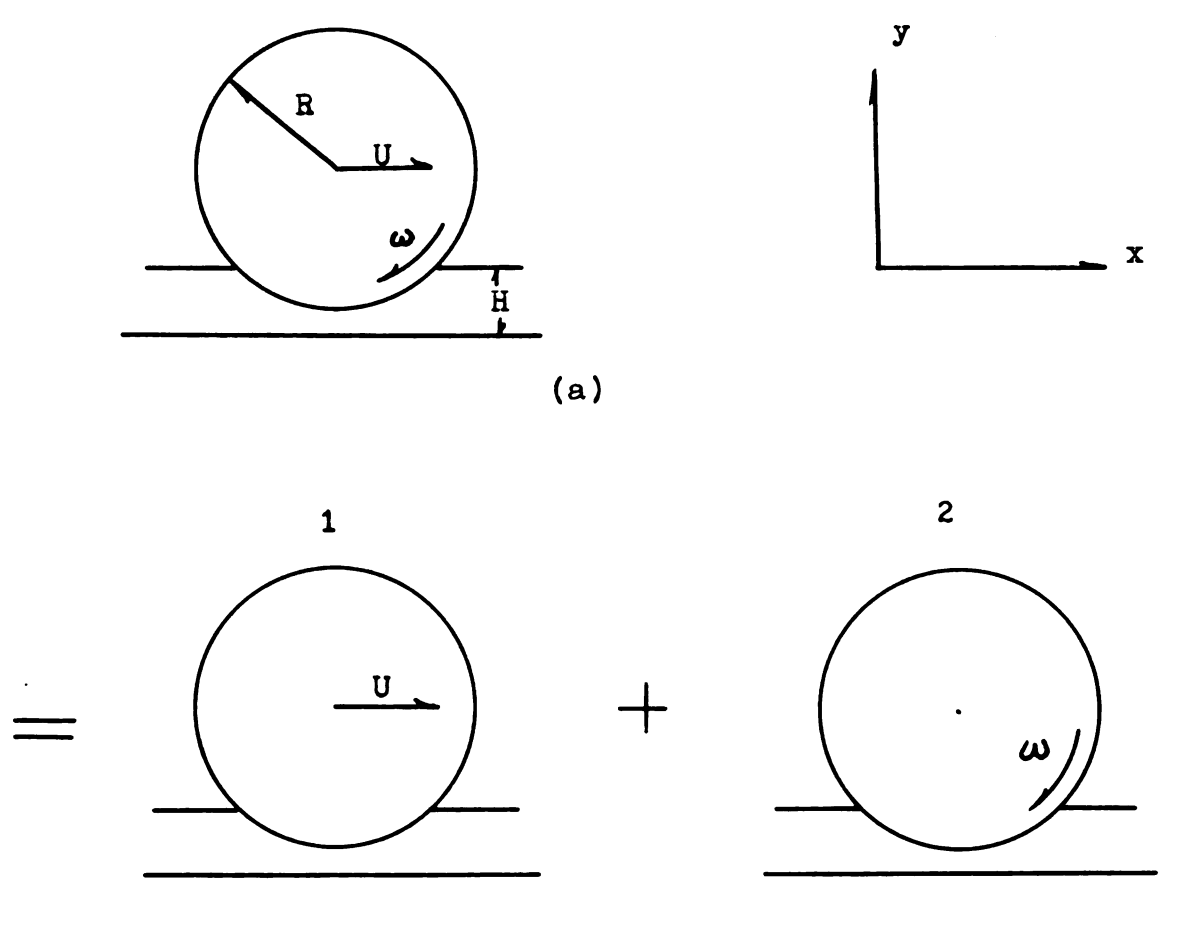
In order to give a clear idea of the characteristics of the velocities, it is helpful to consider U and V separately. Fig. 3, shows the transformation of the velocities U and V.

In Fig. 3;

- (a) is a normal picture of a moving wheel in the viscous film.
- (b) shows U and V separately and relative to the ground.

From here below the velocities are relative to the wheel center.

- (c) 1. shows a flow with a constant velocity -U passing a stationary wheel.
- (c) 2. shows the velocity -V =-ωR of the wheel.
 V is assumed parallel to the ground surface.
- (d) 1. shows the velocity distribution in the fluid caused by the velocity U. In front of the wheel at point a, the distribution of the velocity is a straight line as shown in (d) la. Point b is at the wheel surface where the speed is zero and the velocity distribution is a parabola which is shown by (d) lb. See also Eq. (8).



(b). Relative to ground

or

 $= \frac{1}{-U} + \frac{2}{-V=-R} \omega$

(c). Relative to wheel center

Pig.3: Analysis and transformation of the velocities

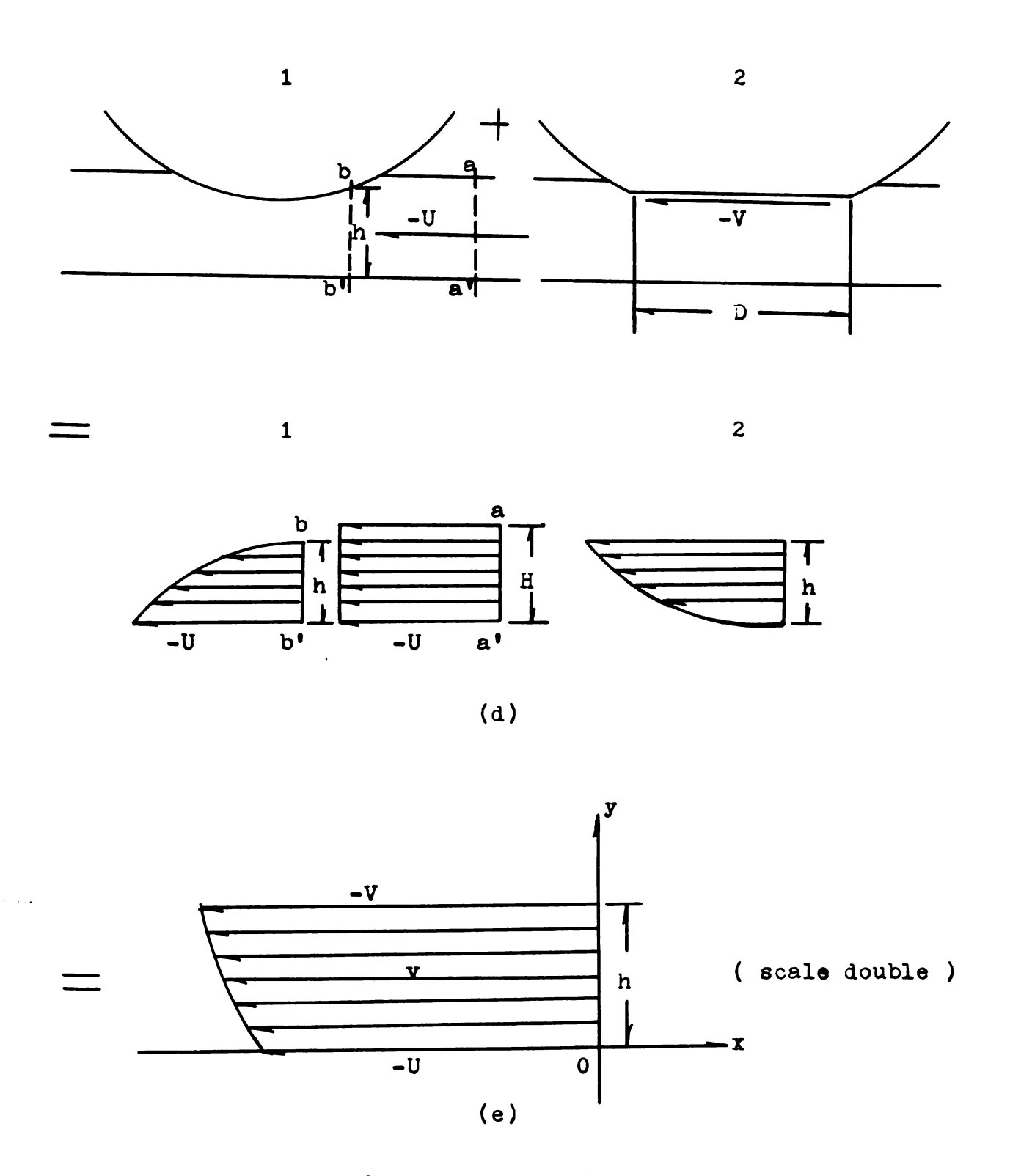


Fig. 3: Analysis and transformation of the velocities (continued)

- (d) 2. shows the velocity distribution of the flow corresponding to -V.
- (e) shows the combination of the velocity distribution of (d) lb and (d) 2 which represents the velocity distribution of this problem.

The absclute values of U and V will usually not be equal. They have a relationship which is stated as

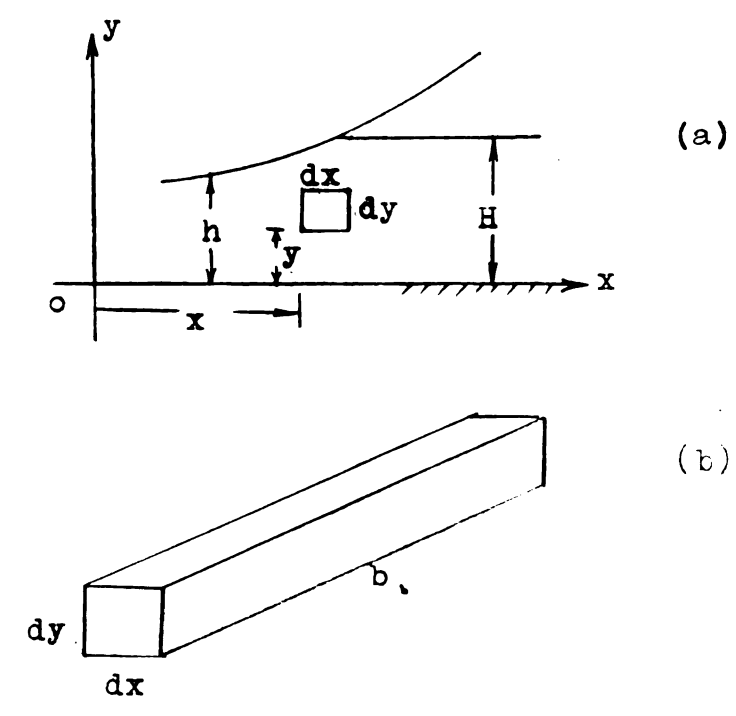
$$\omega R(1-s) = U$$
 or $V = \omega R = \frac{U}{1-s}$ (1) where s is the slip.

If s=0%, no slip exists and $U=V=\omega R$. The velocity distribution under this condition is the same as Fig. 3, (d) la, But, actually, the slip can not be avoided. If s=100%, U=0, which means that the vehicle is "stuck".

By Fig. 3e, the boundary condition of the velocity function, v=F (U,V,h,y,x), under the assumptions they are

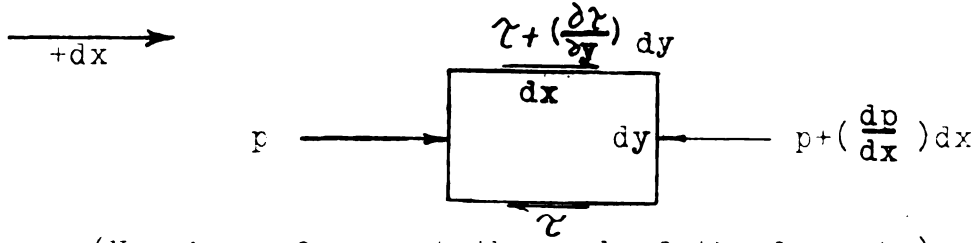
5. The velocity function v=F(U,V,h,y,x)

In the general case, a small element as shown by Fig. 4 is used



Yig. 1. The clement of the fluid.

In Fig. 4b; b is the width of the wheel. The force equilibrium diagram for the element in the x-direction is given by Fig. 5.



(No shear force at the end of the element.)

Fig.5. The forces on the element.

The pressure on the left side area (bdy) of the element is p, and the right side area is p + (dp/dx)dx. The shear stress on the bottom of the element is γ , on the top is $\gamma + (\delta \gamma / \delta y)dy$. The inertia forces resulting from the acceleration of the liquid are small compared to the viscous shear forces and may be neglected.

Set
$$\Sigma F_{x}=0$$

$$\left[p + \left(\frac{dp}{dx}\right)dx\right]bdy + \gamma bdx = \left[\gamma + \left(\frac{\partial \gamma}{\partial y}\right) \cdot dy\right]bdx + pbdy$$

$$\frac{\mathrm{d}\mathbf{p}}{\mathrm{d}\mathbf{x}} = \frac{\partial \mathcal{T}}{\partial \mathbf{y}} \tag{3}$$

By the Newtonian definition of viscosity

$$\mathcal{T} = \mu \frac{\mathrm{d} v}{\mathrm{d} y} \tag{4}$$

As the velocity under the basic assumptions is a function of both x and y, the expression dv/dy in (4) should be changed to $\partial v/\partial y$. The shear stress we are mainly interested in is the stress on the surface of the wheel. For this particular case, the equation (4) should be stated as

$$\mathcal{T}_{\mathbf{h}} = \mathcal{U}(\frac{\partial \mathbf{v}}{\partial \mathbf{y}})_{\mathbf{y}=\mathbf{h}} \quad (\text{Fig. 4a})$$

Differentiate (4)

or

$$\frac{\partial \mathcal{X}}{\partial \mathbf{y}} = \mathcal{M}(\frac{\partial \mathbf{v}}{\partial \mathbf{y}^2}) \tag{5}$$

Combine Eq. (3) and Eq. (5)

$$\frac{\mathrm{d}\,\mathrm{p}}{\mathrm{d}\,\mathrm{x}} = \mu \frac{\delta^2 \mathrm{v}}{\delta \mathrm{y}^2} \tag{6}$$

By solving Eq. (6) the velocity function is found as

$$\mathbf{v} = \frac{1}{2\mu} \left(\frac{\mathrm{d}\mathbf{p}}{\mathrm{d}\mathbf{x}} \right) \cdot \mathbf{y}^2 + \mathbf{v}_1 \mathbf{y} + \mathbf{c}_2 \tag{7}$$

To evaluate the constants C_1 and C_2 , the boundary conditions stated by Eq. (2) are used.

The integration constants are

$$C_1 = -\left[\frac{V-U}{h} + \frac{1}{2\mu}\left(\frac{dp}{dx}\right)h\right]$$

$$C_2 = -U$$

and

$$\gamma - \frac{1}{2\mathcal{H}} \left(\frac{\mathrm{d} p}{\mathrm{d} x} \right) \cdot \left(y^2 - \mathrm{h} y \right) - \left(\frac{\mathrm{V} - \mathrm{U}}{\mathrm{h}} y + \mathrm{U} \right) \tag{3}$$

Eq. (8) shows that the velcelty distribution is a parabolic function in this case, as well as in the ordinary lubrication case. The velocity distribution in Fig. 3e therefore is proved to be a parabola.

6. The general pressure equation

The pressure at points A and A' in Fig. 2 are zero. Furthermore, because the continuity characteristic of the pressure, there must be a maximum pressure point between A and A'. This point will be found where the rate change of the pressure (dr/dx) reaches zero. The velocity at that point is given by Eq. (9)

$$v_0 = -\left(\begin{array}{c} v - v \\ \hline h_0 \end{array}\right)$$
 (9)

where h_{o} is the thickness of the film at the point of.

maximum pressure.

If mainly the middle zone of the film along the x-direction (Fig. 6) is considered, and a very short time interval required for the wheel to pass any section of the film, the sideflow may be neglected and the flow in the x-direction Q, in an unit time, can be assumed constant.

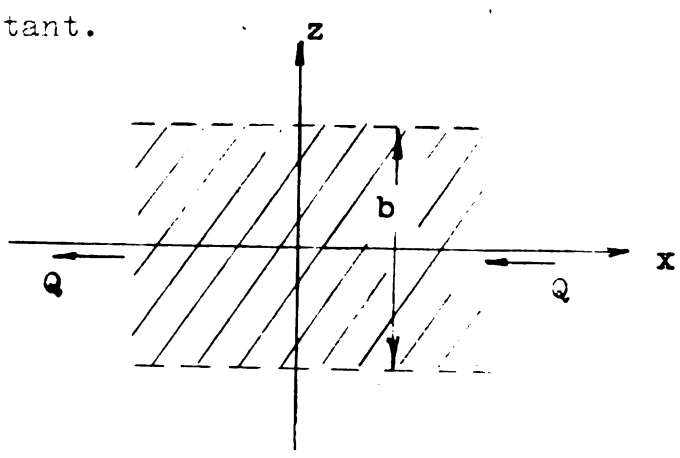


Fig. 6; The gazames dentals given.

Honce.

$$C = \int_{0}^{h} \text{bvdy}$$
 (10)

v is given by Eq. (3), therefore

$$\lim_{x \to \infty} b \int_0^h \left[\frac{1}{2\mu} \cdot \left(\frac{dp}{dx} \right) \cdot \left(y^2 - hy \right) - \left(\frac{V-U}{h} y + U \right) \right] dy$$

$$=-b \left[\frac{1}{12 \mu} \cdot \left(\frac{dp}{dx} \right) h^{3} + \frac{V+U}{2} h \right]$$
 (11)

But dp/dx = 0 at the point where $h \cdot h_0$, Eq. (11) therefore turns out as

$$C = -\frac{U + V}{2} bh_0 \qquad (12)$$

From Eqs. (11) and (12)

$$-\frac{U+V}{2} bh = -b \left[\frac{1}{12\mu} \left(\frac{dr}{dx} \right) h^3 + \frac{U+V}{2} h \right]$$

or

$$\frac{dp}{dx} = 6\mu(U + V) \left[\frac{h_0 - h}{h^3} \right]$$
 (13)

Eq. (13) is the general prossure equation for a moving object with the same velocity characteristics as in this problem. By individually applying this equation to the three regions which are stated in Fig. 2, the pressure profile and total pressure can be found.

7. The lift and friction force equations

Fig. 7 shows a point ${\bf c}$ on the wheel surface which is acted on by two stresses p (pressure) and ${\bf \gamma}$ (shear stress).

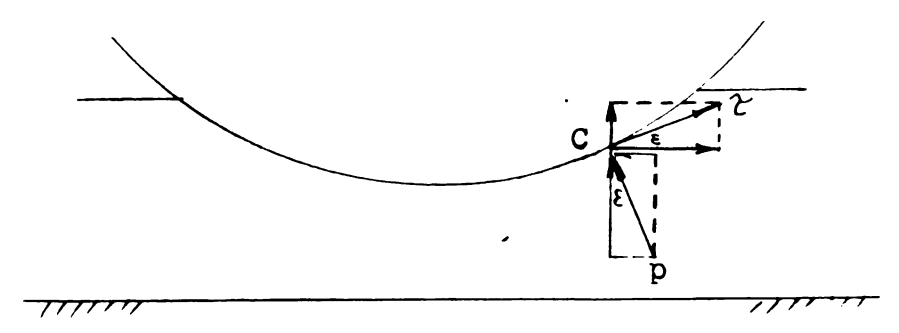


Fig. 7. The forces of any point on the surface of the wheel.

The total lift force P and the friction force F are functions of p and ?,

$$F/b = \int pdx + \mathcal{E} \int rdx$$

$$F/b = \mathcal{E} \int pdx + \int rdx$$
(15)

 \mathcal{E} is the angle shown in Fig. 7 (Because \mathcal{E} in this problem is small, therefore $Sin\mathcal{E}=\mathcal{E}$, $Cos\mathcal{E}=1$ are assumed.) Because there are three regions in this problem, Eq. (15) has three partial solutions. Hence

and
$$P/b = \sum_{i=1}^{m} \left[\int_{p_i} dx + \mathcal{E}_i \mathcal{T}_i dx \right]$$

$$P/b = \sum_{i=1}^{m} \left[\mathcal{E}_i \int_{p_i} dx + \int_{i} \mathcal{T}_i dx \right]$$
(16)

To solve Eq. (16) the values \mathbf{p}_i and \mathbf{T}_i must be

found as functions of x. Eq. (13) gives p_i

$$r_i = 6\mu(U + V) \int (\frac{h_0 - h_1}{h_1^2}) dx$$
 (17)

Mq. (4)' gives

$$\gamma_{i} = (\gamma_{hi}) = \mu(\frac{\delta v}{\delta y})_{y=h}$$

Where ($\delta v/\delta y$) $_{y=h}$ can be determined by rartial differentiating of Eq. (5) with respect to y;

$$\frac{\partial v}{\partial y} = \frac{1}{2\mu} \left(\frac{dp}{dx} \right) \left(2y - h \right) - \frac{y - y}{h}$$

Hence
$$\left(\frac{\partial v}{\partial y}\right)_{y=h} = \frac{1}{2\mu} \left(\frac{dp}{dx}\right)_{h} + \frac{y-v}{h}$$
 (18)

Therefore
$$\gamma_{i} = \frac{1}{2} \cdot (\frac{dp}{dx}) h_{i} + \frac{(U - V)}{h_{i}}$$

$$= \mu \left[3(U + V) \frac{h_{o} - h_{i}}{h_{i}^{2}} + \frac{U - V}{h_{i}} \right] (13)$$

As we assumed that the film thickness is relatively small compared to the radius of the tire, region
(II) will take most lift force and friction resistance.
Therefore the maximum pressure point must exist in this region.

Fig. 8 shows the important elements and assumptions for a tire used for calculating the total lifting force and friction resistance of the wheel. Where, in this figure, \mathbf{E}_1 , \mathbf{E}_2 , \mathbf{E}_3 , are small and we assume

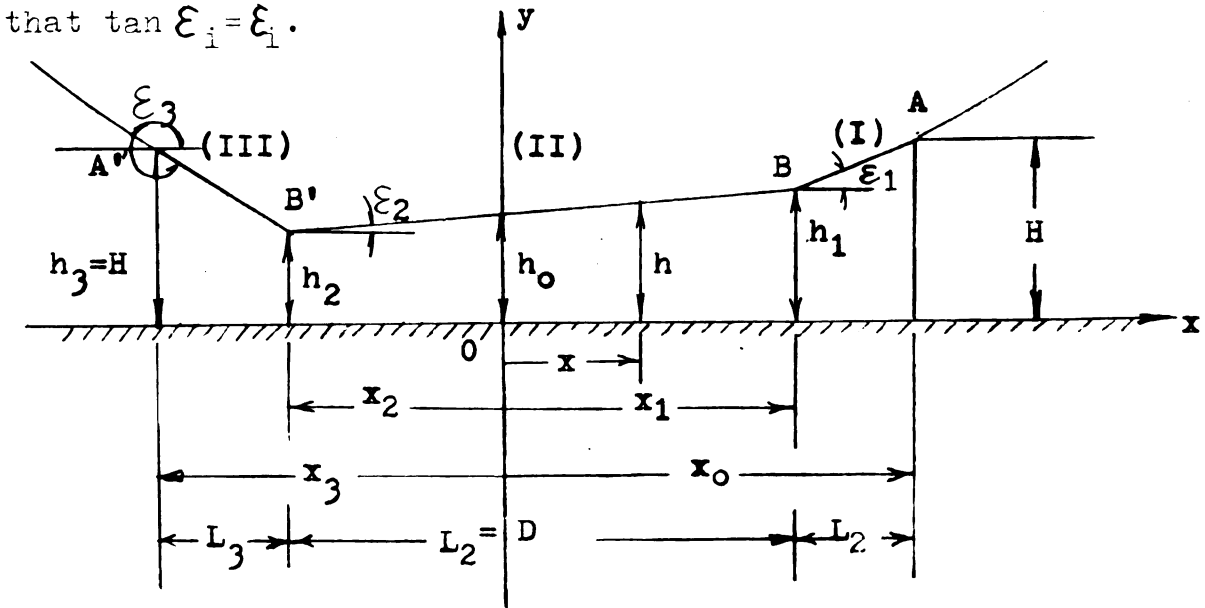


Fig. 8; The deformation of a whoel on the mud film in a x-y coordinate system.

From this figure, we get

$$h_{i} = h_{j} + \mathcal{E}_{j}(\mathbf{x} - \mathbf{x}_{j}), j = 1, 2, 3,$$
Using Eq. (17)
$$p_{i} = 6 \,\mu(\mathbf{U} + \mathbf{V}) \int \frac{h_{o} - \left[h_{j} + \mathbf{\mathcal{E}}_{j} (\mathbf{x} - \mathbf{x}_{j})\right]}{\left[h_{j} + \mathbf{\mathcal{E}}_{j} \cdot (\mathbf{x} - \mathbf{x}_{j})\right]^{3}} d\mathbf{x}$$

$$= 3 \,\mu(\mathbf{U} + \mathbf{V}) \left[\frac{2h_{i} - h_{o}}{\mathcal{E}_{j=1} h_{1}^{2}}\right]$$
(21)

Eq. (16) therefore can be written as $P = \sum_{i=1}^{III} \left\{ 3 \, \mu(U+V) \int \left(\frac{2h_i - h_o}{\mathcal{E}_{j=1}} \right) \, dx \right\}$

$$+\mu\epsilon_{i}\left\{3\left(U+V\right)\frac{h_{o}-h_{i}}{h_{i}^{2}}+\frac{U-V}{h_{i}}\right\}dx\right\} \tag{22}$$

and Eq. (17) becomes $F = \sum_{i=1}^{\mathbf{HI}} \left\{ 3\mu(\mathbf{U} + \mathbf{V}) \mathcal{E}_{i} \right\} \left(\frac{2\mathbf{h}_{i} - \mathbf{h}_{o}}{\mathcal{E}_{j=i}\mathbf{h}_{i}} - \mathbf{U}_{i} \right) d\mathbf{x}$ $+ \mu \int \left[3 \cdot (\mathbf{U} + \mathbf{V}) \frac{\mathbf{h}_{o} - \mathbf{h}_{i}}{\mathbf{h}_{i}^{2}} - \frac{\mathbf{U} - \mathbf{V}}{\mathbf{h}_{i}} \right] d\mathbf{x}$ (23)

The boundary conditions for Eqs. (19) and (21) are

a), For
$$x=x_0$$
: $H=h_1+\boldsymbol{\xi}_1L_1$; $(p_1)=0$
b), For $x=x_1$: $h_1=h_2+\boldsymbol{\xi}_2L_2$; $(p_1)_{x=x_1}=(p_{II})_{x=x_1}$
c), For $x=0$: $h_0=h_2-\boldsymbol{\xi}_2x_2$;
d), For $x=x_2$: $h_2=h_3+\boldsymbol{\xi}_3L_3$; $(p_{II})_{x=x_2}=(p_{III})_{x=x_2}$
e), For $x=x_3$: $h_3=H$ $(p_{III})=0$

These boundary conditions for p_i makes it possible to solve C_i and h_o , h_j , two ξ_j can then be solved. Eq. (22) gives the remaining ξ_j . The results will be functions of L_i , H, μ and velocities U and V.

8. A calculation example

In actural case, the pressure in Region I and III are small compared to Region II. If we consider that the pressure in Regions I and III are negligible, and omit the y-direction component of the friction resistance it will simplify a great deal of calculation for finding the lifting force in Region II. This lifting force will represent approximately the total lifting force caused by the relative motion of the wheel.

By this assumption, from Fig. 9, the boundary conditions of the pressure p in Region II are

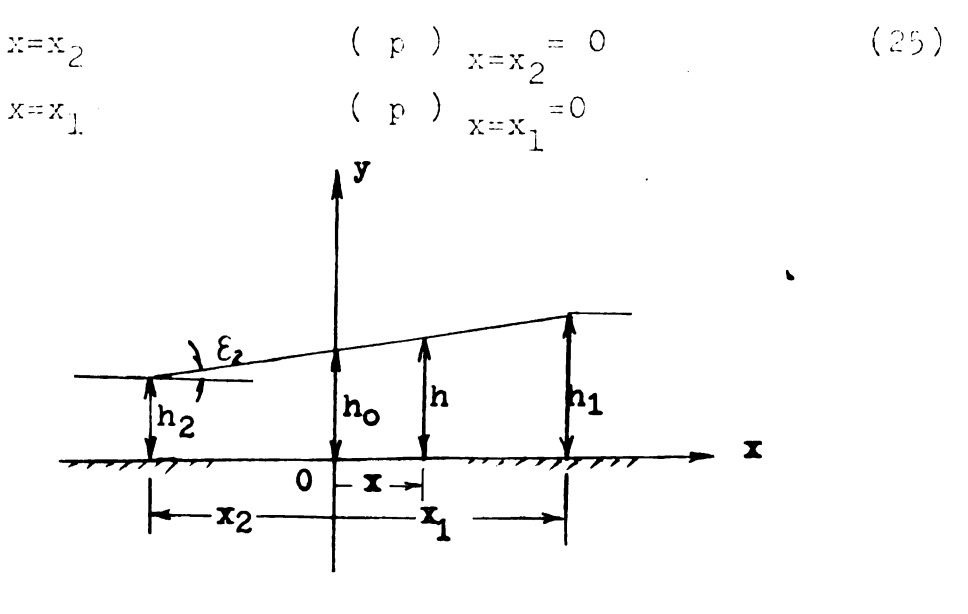


Fig. 9. Simplified diagram of Fig. 8. for calculation example.

From the figure, we get

$$h = h_2 + \xi_2 (x - x_2)$$

Eq. (21) therefore becomes
$$p_{i}=p=3\mu (U+V) \left\{ \frac{2 \left[h_{2} + \mathcal{E}_{2} (x-x_{2}) \right] - h_{0}}{\mathcal{E}_{2} \left[h_{2} + \mathcal{E}_{2} (x-x_{2}) \right]^{2}} + C_{II} \right\}$$
(26)

Substituting Eq. (25) into Eq. (26), we get

$$\frac{2(h_2 + \mathcal{E}_2 D) - h_0}{(h_2 + \mathcal{E}_2 D)^2} + C_{II} = \mathbf{0}$$
 (27)

$$\frac{2h_2 - h_0}{\xi_2 h_2^2} + c_{II} = 0$$
 (28)

Solving Eqs. (27) and (28), we obtain
$$h_0 = \frac{2h_2 \cdot (h_2 + \xi_2 D)}{2h_2 + \xi_2 D}$$
(29)

$$c_{\text{II}} = -\frac{2}{\mathcal{E}_2 \left(2h_2 + \mathcal{E}_2 D\right)} \tag{30}$$

Substituting Eqs. (29) and (30) into Eq. (21), we get

$$p = \frac{3\mu(U+V)}{\varepsilon_2} \begin{bmatrix} 2h_2 \cdot (h_2 + \varepsilon_2 D) \\ -\frac{2h_2 \cdot (h_2 + \varepsilon_2 D)}{2h_2 + \varepsilon_2 D} \\ -\frac{2h_2 \cdot \varepsilon_2 D}{2h_2 + \varepsilon_2 D} \end{bmatrix}$$
(31)

The total lift force is

$$F = b \int_{x_2}^{x_1} p dx$$

$$=\frac{6\mathcal{M}(\mathtt{U}+\mathtt{V})\ \mathtt{b}}{\boldsymbol{\mathcal{E}}_{2}^{2}}\left\{\begin{array}{cc} \log\frac{\mathtt{h}_{2}+\boldsymbol{\mathcal{E}}_{2}\mathtt{D}}{\mathtt{h}_{2}} & -\frac{2\mathtt{D}\boldsymbol{\mathcal{E}}_{2}}{2\mathtt{h}_{2}+\boldsymbol{\mathcal{E}}_{2}\mathtt{D}} \end{array}\right\}$$

Because $h_1 = h_2 + \xi_2 D$,

$$P = \frac{6\mu(y+y) b}{\epsilon_{2}^{2}} \left\{ \frac{\log h_{1}}{h_{2}} - \frac{2(h_{1} - h_{2})}{h_{1} + h_{2}} \right\} (32)$$

In Eq. (32), the value F depends on the ratio of h_1/h_2 . If we assume $h_1/h_2 = 1.1o$, we get $h_1 + h_2 = 2.10h_2$, and $h_1 - h_2 = 0.10h_2$, $\boldsymbol{\mathcal{E}}_2^2 = 0.01 \, \boldsymbol{h}_2^2 / \boldsymbol{D}^2$. Substituting these values into Eq. (32) gives

$$F = 0.06 \mu(U+V) bv^2 - \frac{1}{h_2^2}$$
 (33)

The values of μ , U, V, b, D and P for a common tire can be assumed as follows

$$\mu = 47 \text{kl}0^{-6} \text{ lb-ses/in}^2 \text{ (Hogedus 1955)}$$

$$V = 15mph = 264 in/sec.$$

$$s = 50\%$$

$$U = sV = 132 \text{ in/sec.}$$

$$D = 10 in.$$

$$b = 5 in.$$

Hence

$$h_2^2 = \frac{0.06 \times 47 \times 10^{-6} (264 + 132) 5 \times 100}{2000}$$

$$= \frac{0.558}{2000}$$

 $= 0.000279 in^2$

Therefore

 $h_2 = 0.0167 ip.$

This value seems reasonable when compared to the result of the experiment which is stated on page 49.

BLAT II

EXPERIMENTAL WORK

(The viscosity of the mud film)

9. Review of Literature on the Viscometers

Several methods have been developed to measure the absolute viscosity. The method we are interested in is the rotational viscometer which includes coaxial-cylinder type, cone-plate type, disk type and conicylinder type.

The coaxial-cylinder type is shown schematically in Fig.10. A cylinder of radius $R_{\rm b}$ is suspended in the sample fluid with the submerged height h in a container of radius $R_{\rm c}$. The inner cylinder, or core, rotates with a constant angular velocity ω in the outer cylinder.

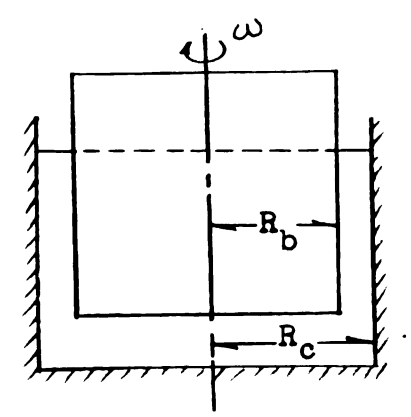


Fig. 10. The coaxial-cylinder type viscometer

Several designs of this type are listed as following; (Wazer 1963)

(a). MacMichal Viscometer

It has a motor-driven cup in which a cylinder of slightly smaller diameter is suspended. The motor drives the cylinder and the viscous drag of the liquid is balanced by the torque of the suspended wire. The test

reading has to be made as soon as the cylinder reaches equilibrium position.

(b). Stormer Viscometer

This viscometer is similar to the MacMichal's but cylinder is much smaller than the cup and driven by a wire and a weight. The cup containing the sample is raised until the cylinder is submerged. A reading is taken of the time required for 100 revolutions of the cylinder as indicated by the revolution counter above the cylinder. •

(c), Brookfield Viscemeter

This viscometer can only obtain the relative value. The viscosity is measured as the torque required to rotate a cylinder or disk at constant speed in a large beaker of the test liquid. A scale indicates the torque transmitted to the spindle as a measure of viscosity.

Some more **v**iscosity measurement instruments of this type are the Rotovisco, the Folarad, the Fann V-G and the Hercules High-Shear viscometers. (Wazer 1963)

The cone-and-plate type is shown in Fig. 11. The appealing feature of the plate-and-cone principle is that for small angles ($\propto <$ ca.3°) the rate of shear across the conical gap may be considered constant and therefore $\omega/_{\propto}$ gives directly the true rate of shear.

$$\mu = \frac{3 \propto M}{2 \pi R^3 \omega}$$

The Rheogoniometer and the Ferranti-Shirly Viscometer are this type. (Wazer 1963)

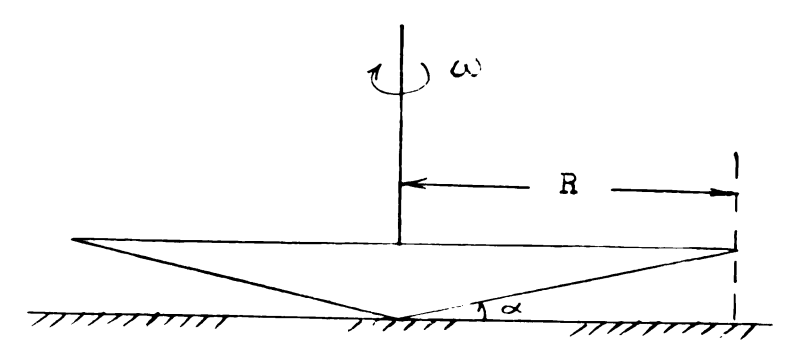


Fig. 11. Come-plate viscometer

The disk type viscometer is shown by Fig. 12. It consists of a very thin disk rotating between two equally spaced parallel plates. The disk is separated from these plates by the distance ℓ . The Brookfield Synchro-Lectric, and the Mooney viscometers are of this type (Wazer 1963).

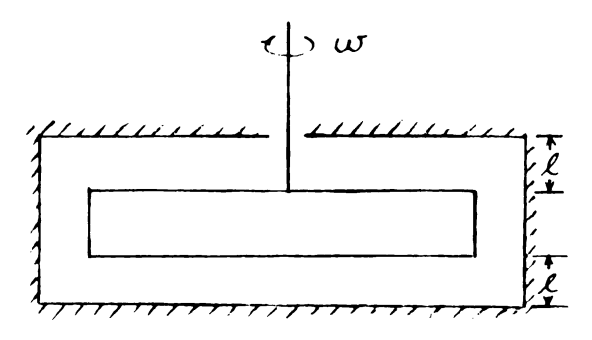


Fig. 12. Disk viscometer.

Fig. 13 shows the principle of a <u>coni-cylindrical</u> <u>viscometer</u>. Several commercially available instruments have used modifications of this design. The

advantage of the combined coaxial cylinder and conical viscometer is that the mean rate of shear in the cylindrical annulus and in the conical portion is about the same and the end effect is nearly eliminated.

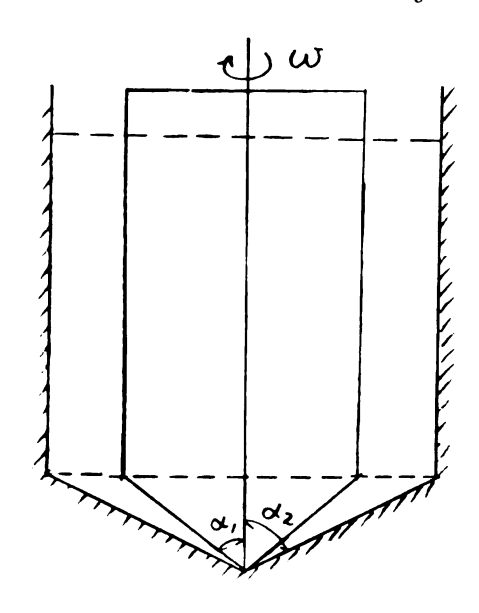


Fig. 13. Coni-cylindrical viscometer

All in all, responses of the rotating disk or conicylindrical viscometer are somewhat less understood.

The conceplate viscometer has the attractive feature of giving constant rate of shear across the gap; therefore equations for this instrument are simple when the angle is kept small. For this reason the cone-and-plate viscometer is becoming more popular with researchers studying non-Newtonian fluid.

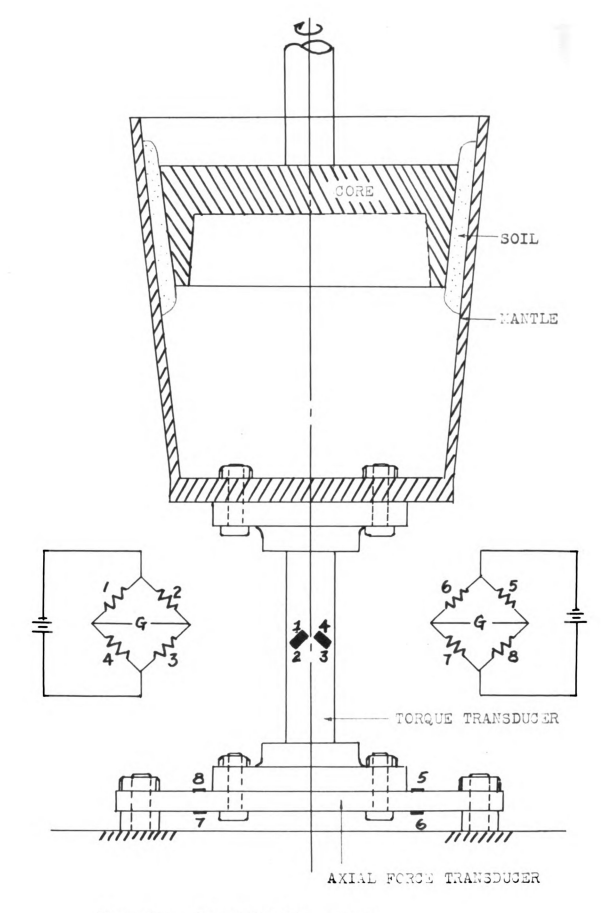


Fig. 14: The CONE Viscometer

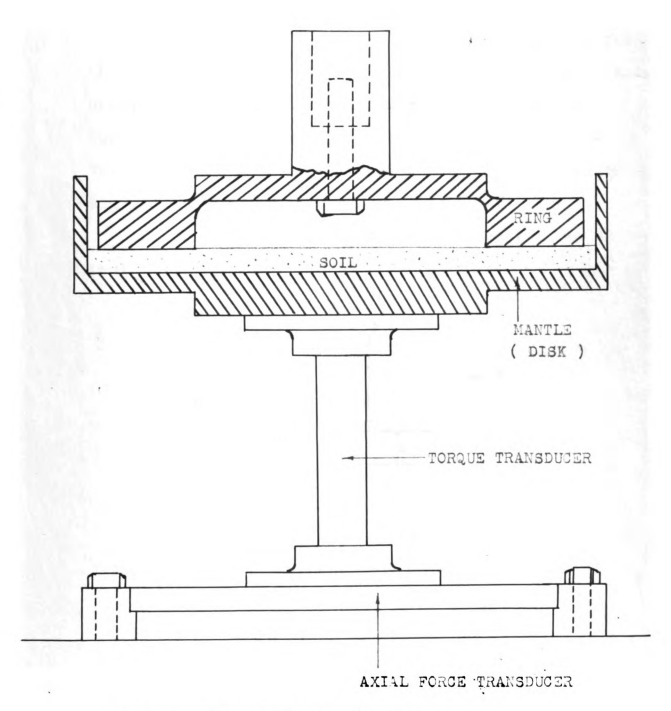


Fig. 15: The Ring-disk Viscometer

10. The Cone Viscometer and the Ring-disk Viscometer

The viscometers now available are not designed for the purpose of measuring the viscosity of mud, especially under the condition which is assumed in this study.

Two types of viscometers were developed, namely Cone

Viscometer and Ring-disk Viscometer which are shown by

Fig. 14 and Fig. 15.

The design of the viscometers Fig. 16 follows the basic assumptions.

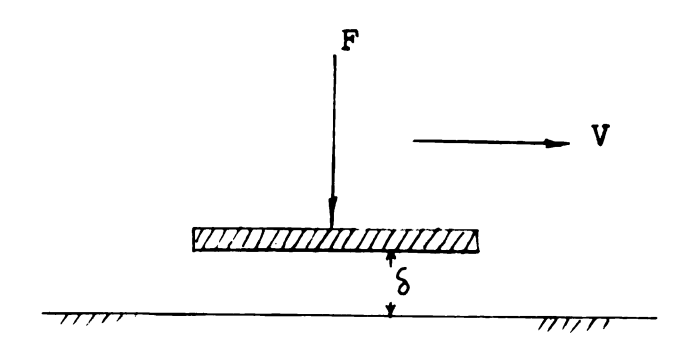


Fig. 16; The principle of the viscometers

F is normal lead, V is the travel velocity, S is the film thickness. The viscometers were mounted on the bed of a vertical milling machine. The bed can be moved vertically and horizontally by two correspondent cranks—which are shown in Fig. 17.

Strain gages were used to measure the torque and axial force and the clearance. The torque and axial force transducers are also shown in Fig. 14.

A Brush Six Channel Oscillograph (Model BL 266) was used with three Brush Amplifiers (Model BL 520, BL 320 and RD 5612), one each for torque, axial force and clearance transducers. Fig. 17, 18, 19 and 20 show the details of the Ring-disk Viscometer and its operation.

In the viscometer, the core, or ring, corresponds to the wheel which slips over the soil and exerts a certain pressure equal to the contact pressure between the tire and the rigid ground. The soil used (a heavy clay) was mixed with water to a moisture content corresponding to the plastic limit. The soil then was applied in the mantle in a uniform layer about 1/2 in. thick. After a smooth surface was formed by pressing the core, or ring, towards the mantle the soil was allowed to dry. Two soil conditions were tested. One was with the moisture content about the shrinkage limit of the soil which was estimated about 10%. The other was with an air dry soil which was estimated about 2%. A sufficient amount of water was applied to the soil surface in order to make it running with water. the core, or ring, was started and the soil was lifted up against it.

The Cone Viscometer failed to build up the pressure



Six channel oscillograph

Amplifiers

Horizontal movement crank

Axial increment crank

Fig. 17. Total view of the viscometer



Fig. 18. Soil sample prepared before test



Fig.19. Viscometer in testing position



Contact area

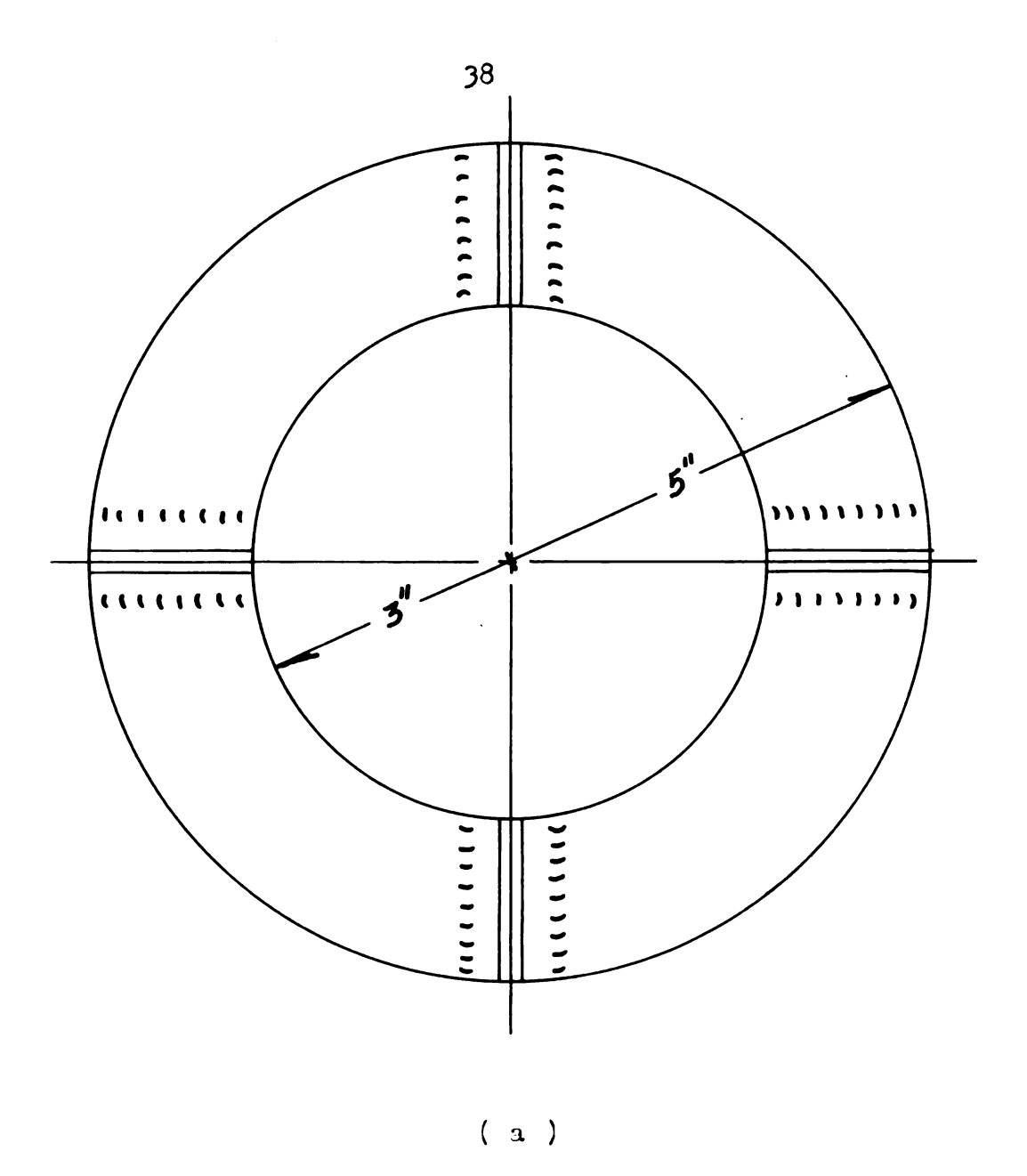
Fig. 20. Sample after test

we desired. The reason was that the soil was deformed too fast and was squeezed out of the contact area before the pressure was built up. The dry soil provided a hard bed which was not squeezed out but the shrinking caused the soil sample to loosen from the mantle and rotate with the core.

The Ring-disk Viscometer gave more satisfactory results not only on the building up the pressure but also on maintaining the water film in the contact area. The only disadvantage was that the relative velocity is not constant, but the average velocity should give an acceptable value.

The test results on Ring-disk Viscometer showed that both pressure and torque curves had a pronounced peak. This made it difficult to read the exact value, especially the torque value corresponding to each pressure peak. This was attributed to a breakdown in the lubricating film. Therefore, in order to obtain a more constant torque reading, four lubrication grooves were made on the ring as shown in Fig. 21. This gave the water a better chance to get into the contact area and maintain a constant thickness of mud film between the two surfaces.

11. Procedures of Operating the Ring-disk Viscometer. In order to obtain the value of μ , the film



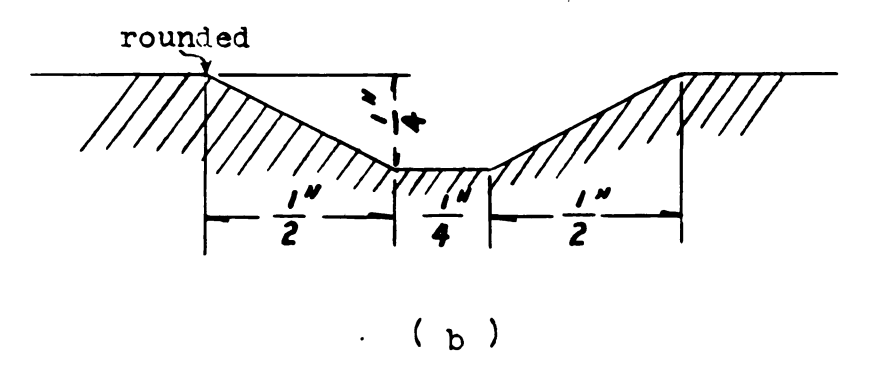


Fig.21; Lubrication grooves on the Ring-disk Viscometer

thickness of must be determined. The strain gaged movement indicator did not give enough accuracy and was used only to record that the bed had been moved. The size of the move was determined from the vertical movement screw of the milling machine, which was graduated in 0.001 inch.

In detail, the procedure of obtaining the torque, axial force and film thickness is as follows:

- (1). The soil sample was prepared with the surface as flat as possible.
- (2). The soil surface was wetted to build up a wet surface. The ring was run for a certain period of time to make the soil surface smooth.
- (3). The ring was run at 50rpm and the zero wear point was determined by raising the mantle up against the ring until the recorder showed a pressure.
- (4). The mantle was raised 15 scale readings (0.015 in) for 1-2 second and then lowered to 0 again. This was repeated five times and then the zero point was determined again. This gives the value of the wear, the axial forces and the corresponding torques.
- (5). Came steps as 3 and 4 but with 25 scale readings.
- (6). Same as steps 3 and 4 but with 35 scale readings.
- (7). Change the rotation speed to 150rpm and repeat steps 3, 4, 5 and 6 once.
- (8). Change the rotation speed to 450 rpm and repeat steps 3, 4, 5 and 6 once.

For each test some soil was worn off the solid soil which had to be compensated for. Under the influence of the normal load the device had an elastic deflection which also had to be taken in account. The following equation was used.

Scale readings - Wear of soil + Film thickness

= Elastic deflection + Initial film thickness (34)
The elastic deflection was determined with no rotation
and is shown in Fig. 24 curve a. Wear is the difference
between the zero points before and after a series of
tests.

12. Results, Discussions and Conclusions

Two sets of data were obtained from two soil conditions (condition 1 is the sample with initially estimated 10% moisture content which corresponds to the shrinkage limit of the soil and condition 2 is air dry soil). Fig. 22 a, b and Fig. 23 a, b were plotted for shear stress (τ) vs. normal pressure (τ) to represent the conditions 1 and 2 respectively. In these figures, a group of 4 or 5 or 6 points obtained from a same increment of scale readings were connected by a line. This showed the variation properties of the data and gave a better understanding of the test results.

Fig. 22 and Fig. 23 showed that the shear stress (7) increased linearly with normal pressure and that

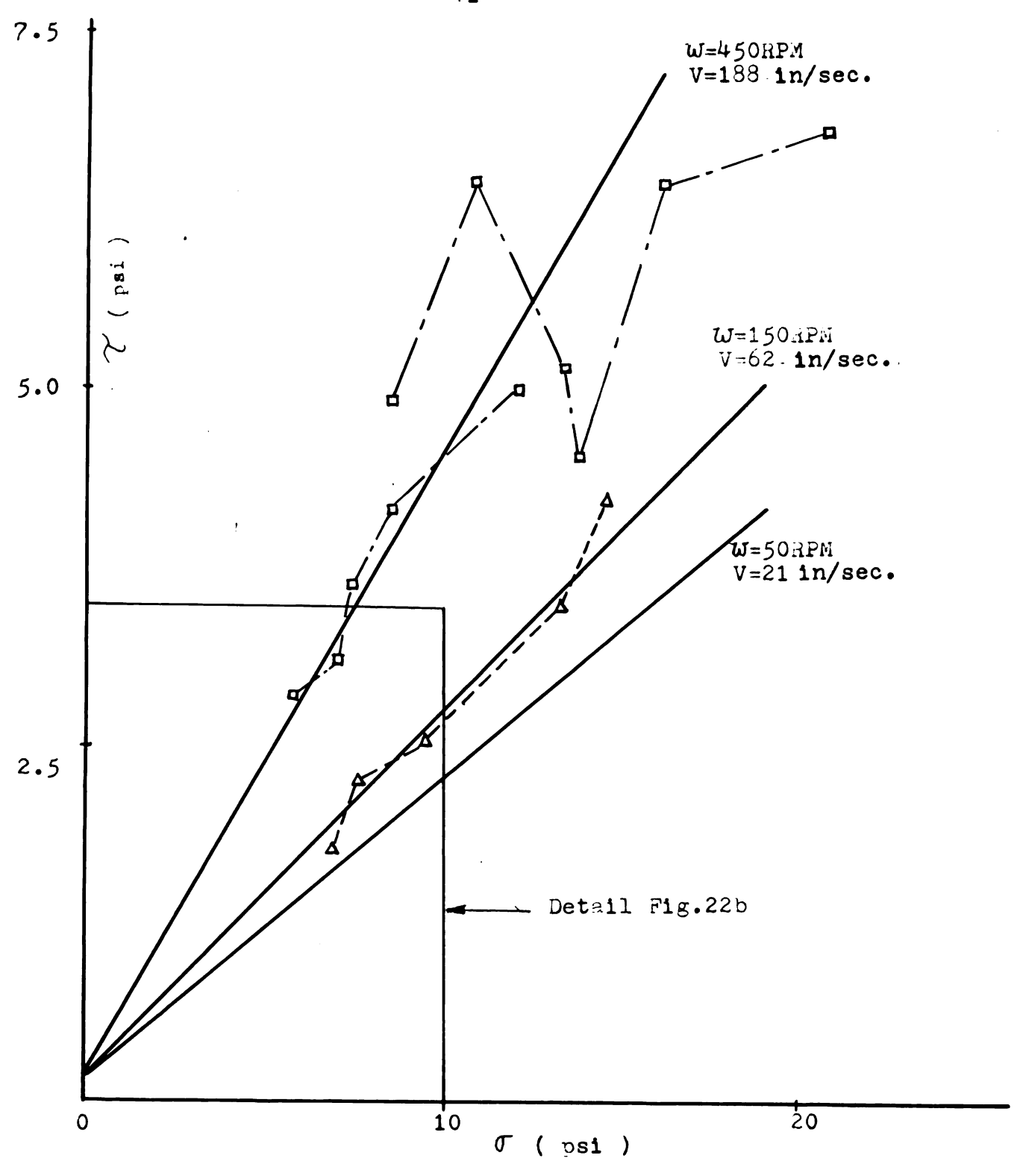
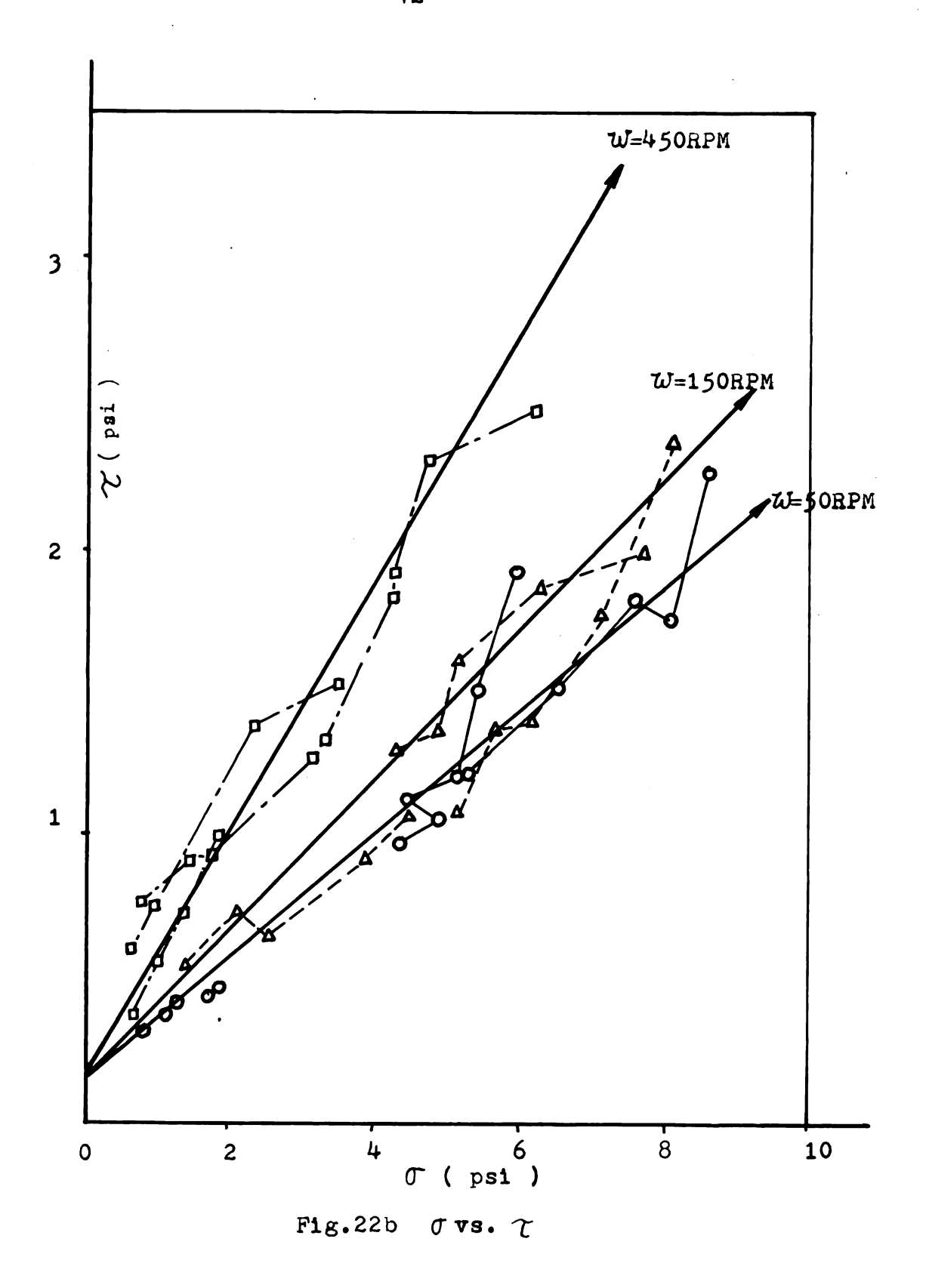


Fig.22a Normal pressure (σ) Vs. Shear stress (\mathcal{T}) (Soil Condition 1)



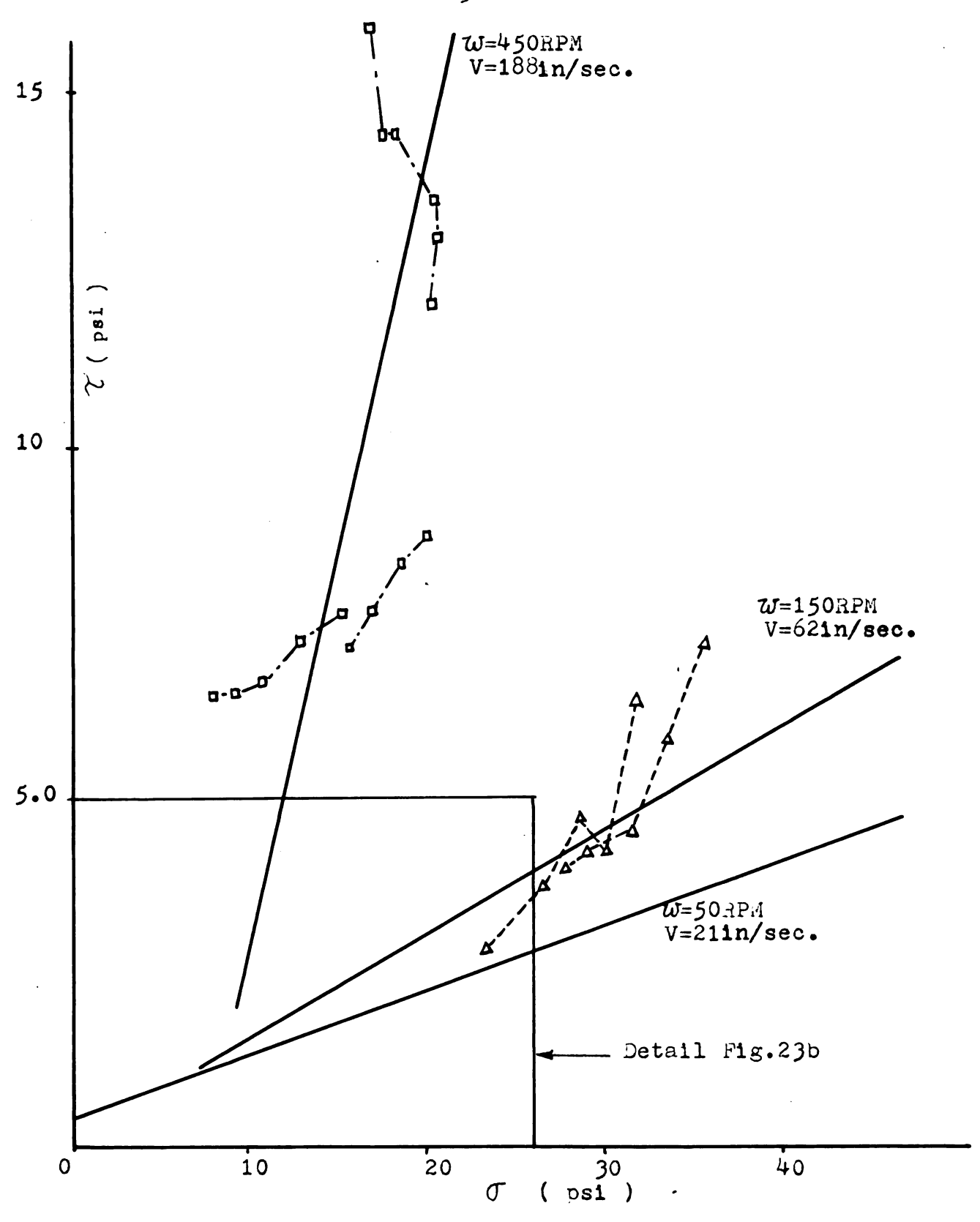
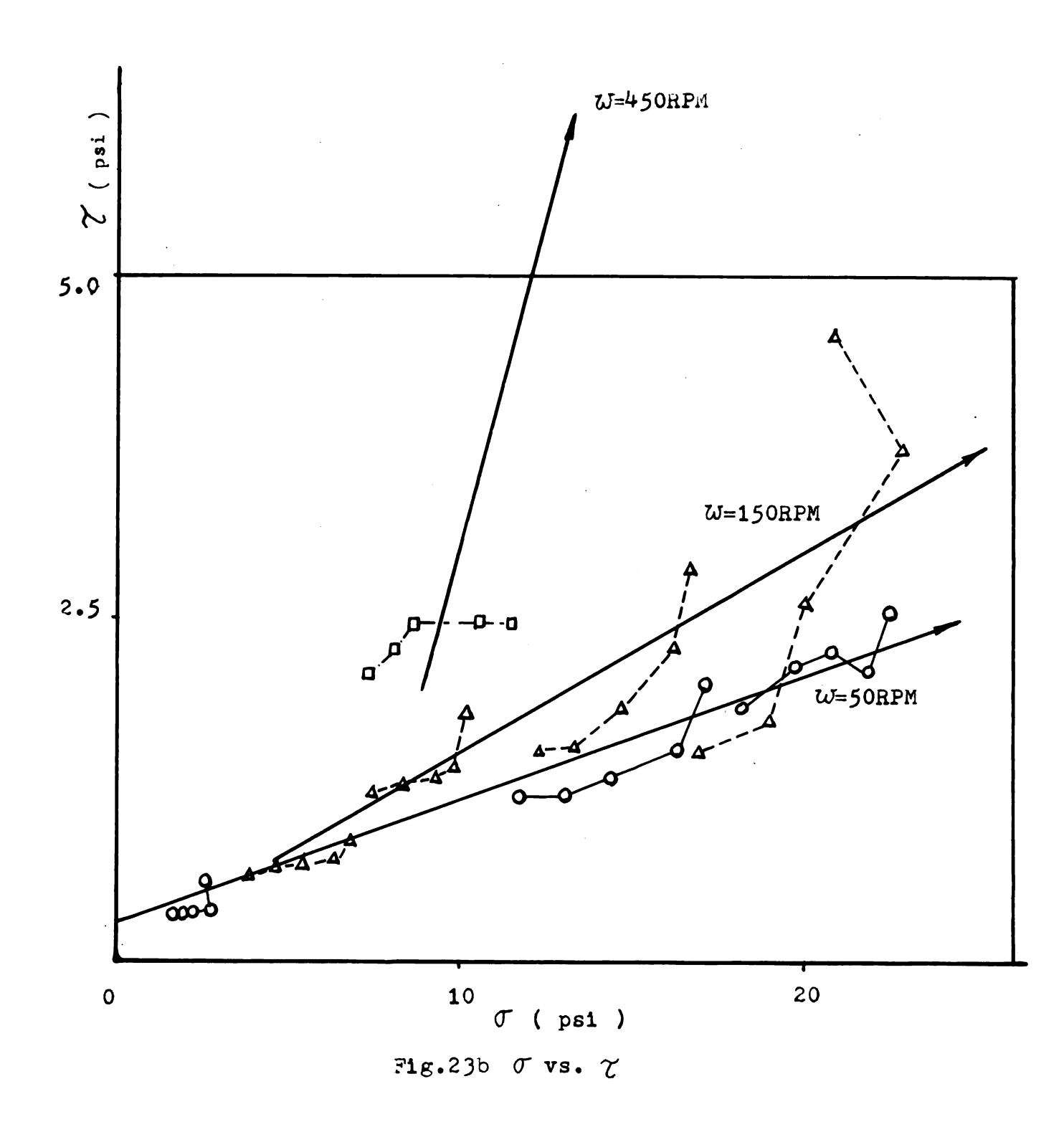


Fig.23a Normal pressure (σ) Vs. Shear stress (γ) (Soil Condition 2)



the increase was larger when velocity increased. By comparing the two figures, we found that, for the same velocity the slope of the lines differed between the two soil conditions. One of the reasons for this probably is that the initial meisture content of these soils were different. The air dry soil was much harder than the soil with shrinkage limit moisture content. The normal pressure produced a higher shear stress under the air dry soil condition.

Because the slope of the lines in Fig. 22 and Fig. 23 changed with respect to velocity, there must be a positive effect of the velocity on the shear stress, in other words a viscous effect. This means that for a given load, a vehicle can obtain a greater pull when its slip speed (V = V) is increased.

In order to find the constants for this influence, a multiple regression has been run on the computer CDC 3600 using program COME. This program was based on the equation

$$\mathcal{T} = a + b\sigma + c \frac{V}{\delta}$$
 (35)

where a is a constant corresponding to adhesion

b is the coefficient of friction

c is the absolute viscosity μ .

? is the shear stress

S is the film thickness

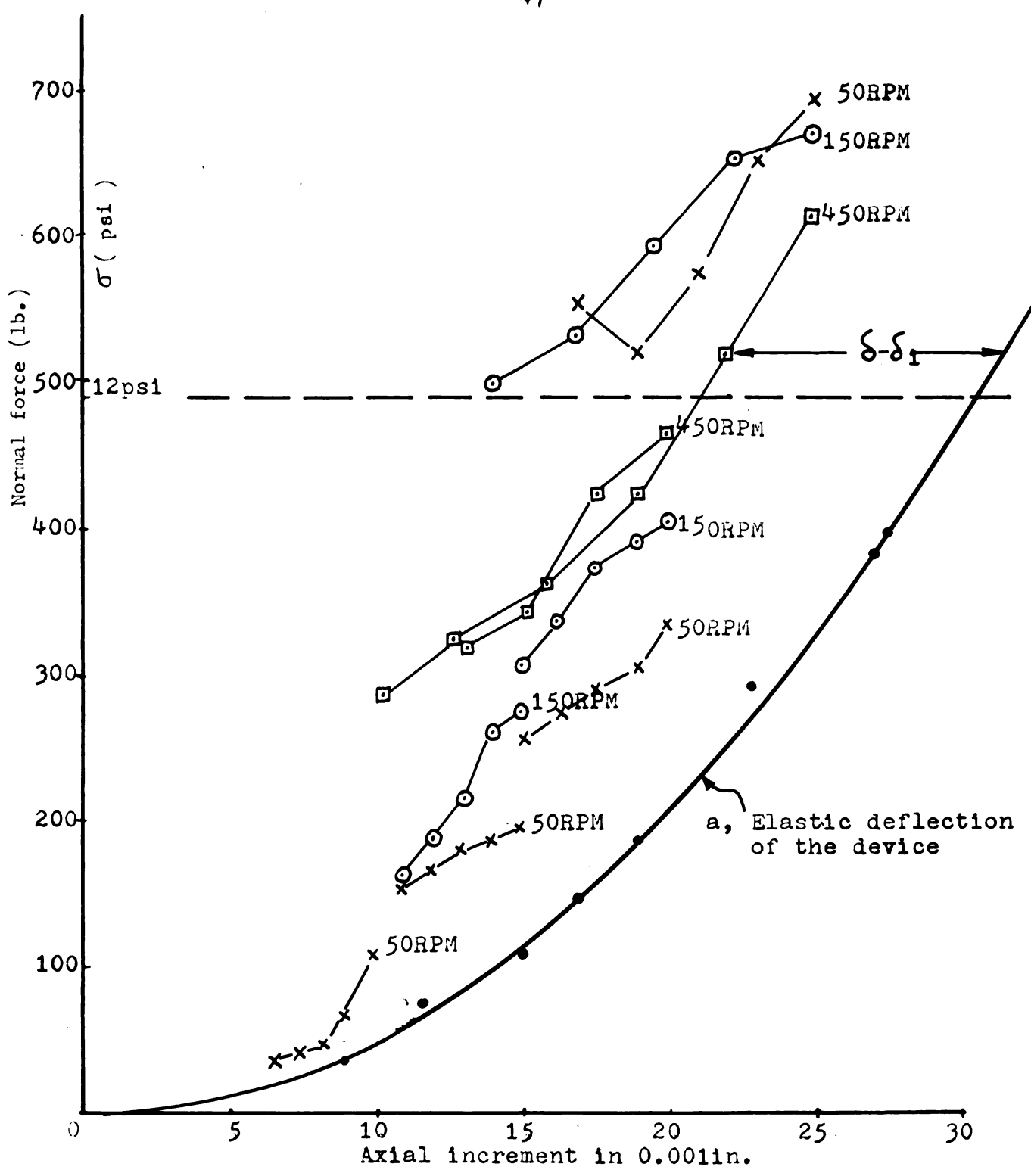
 σ is the normal pressure V/S is the velocity gradient

The value μ was found between 0.000005 and 0.000175 lb-sec/in². This is in fairly good agreement with the values given by Hegedus (1958).

However, since the standard errors were very large, the values obtained from the computer calculation should not be used for further calculations. In order to find the reason for the inaccuracy, we checked the data of soil conditions 2 and 1 in detail and plotted the film thickness (8) vs. normal pressure (σ) in Fig. 24 and Fig. 25 respectively. In these figures, the same method of expressing the data as in Fig. 22 and Fig. 23 was used. The corresponding velocity is stated at the first point of each set. It shows how the normal pressure decreases when the soil is worn off the solid surface.

Fig. 24 was divided into two parts by the 12psi normal pressure line. Above or below this pressure, each part agreed with the lubrication theory in so far that a greater clearance was formed for a higher speed. The reason why this did not hold true when comparing across the 12psi line could not be found, therefore, further investigation is necessary on this point.

Another discrepancy is that the film thickness increases for increasing load if two sets of measurements are



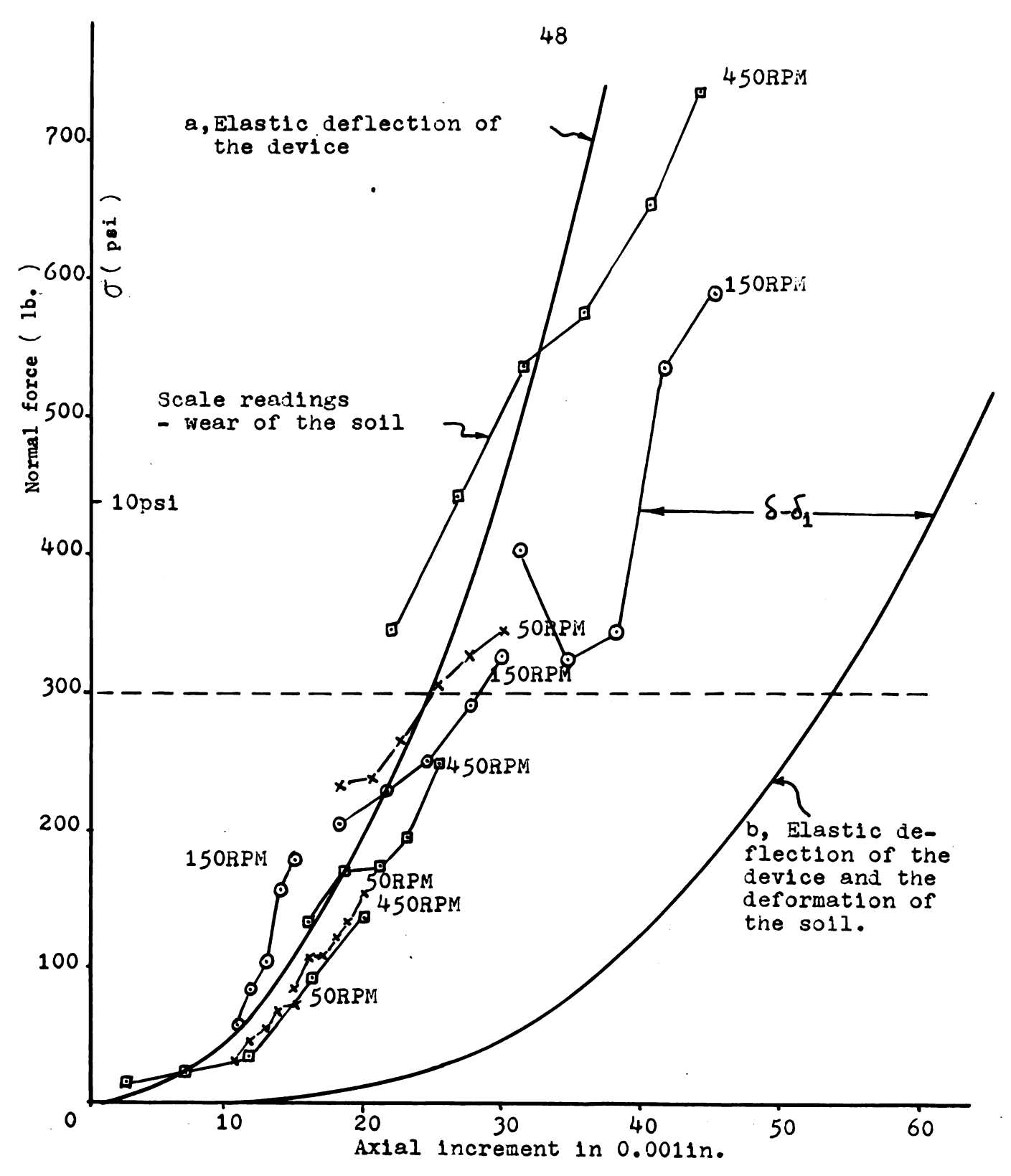


Fig.25 Film thickness (δ) vs. Normal pressure (σ) (Soil condition 1) $\delta_{\bf i}$ is the initial film thickness

compared but not within a set of measurements. This indicates an inaccuracy in the determination of the film thickness.

In Fig. 25, we used curve b as the reference line, because we found that the soil deformed a large value when the normal pressure was applied. Curve b is the calibration curve of the elastic deflection of the device and the deformation of the soil. In this figure, the relationship of the sets are not so clear as that in Fig. 24. They do not agree with the lubrication theory as far as the velocity and the film thickness are concerned. But within each set of measurement, it agrees with the lubrication theory when the normal pressure is greater than 8 psi and disagrees with the theory when the normal pressure is less than 8 psi. This again indicates an inaccuracy in the determination of the film thickness.

Comparing the results from the calculation example and the experiment, we obtained an interesting result. In the example we assumed that $\sigma = 40 \, \mathrm{psi}$, V-U =132 in/sec (slip speed) and obtained $\delta = 0.0167$ in. From Fig. 24 $\delta = 0.010$ in. for the speed 188.6 in/sec and $\sigma = 13 \, \mathrm{psi}$. This indicates the calculated value given in the early part of this thesis might give a reasonable result.

In the further investigations, the test of the viscosity by the Ring-disk Viscometer could be improved in the following manner

- (1). More accurate determ ination of the elastic deflection of the device and the soil is necessary.
- (2). More accurate determination of the zero clearance between ring and soil sample surface is necessary.
- (3). A continuous water supply system should be arranged to give a better chance to maintain the mud film between ring and soil sample surface.
- (4). The temperature influence should be checked. Temperature might become a problem when the rotating speed is high and the normal pressure is large.
- (5). The instrumentation should be improved regarding
 - i, Better design of the clearance transducer
 - ii, Stabilizing the pen when the attenuation is small
 - iii, Zero point of the pen when the attenuation is changed.

٠.

iv, Bridge balance.

REFERENCES

- 1. Aronson, M. H. and Nelson, R. C. (1964) "Viscosity Measurement and Control." Instruments Publishing Company,
 Inc. Pittsburgh, Pa.
- 2. Baver L. D. (1963) Soil Physics John Wiley & Sons, Inc., New York.
- 3. Bekker, M. G. (1956) * Theory of Land Locomotion * University of Michigan Press. Ann Arbor.
- 4. "Brush Six Channel Dynamic Recorder ", "Oscillgraph ",
 "Input Box ", "Amplifier ". Brush Electronics Company.
- 5. Czako, T. and Hegedus E. (1958) * Physical Soil and Snow Values for the Determination of Vehicle Motion Resistance.* A Soil Value System for Land Locomotion Mechanics. Res. Report No.5, Center Line, Michigan.
- 6. Dobie, W. B. and Peter, C. G. (1948) * Electric Resistance Strain Gauges.* John Wiley & Sons, Inc., New York.
- 7. Eirich, F. R. (1956, 1958, 1960) * Rheology * Vol.I, II, III. Academic Press, New York.
- 8. Fuller, Duolly D. (1956) "Theory and Practice of Lubrication for Engineers." John Wiley & Sons, Inc., New York.
- 9. Harrison, W. L. (1957) A Study of Snow Values Related to Vehicle Performance. Research Report No.23, Land Locomotion Research Branch, Center Line, Michigan.
- 10. Hegedus, E. (1958) * Drag Coefficients in Locomotion over Viscous Soils (Wheels)* Land Locomotion Research Branch,

- Research Report No.25, Center Line, Michigan.
- 11. Hegedus, E. (1958) "Wheels in Viscous Mud." A Soil

 System for Land Locomotion Mechanics, Research Report

 No.5, pp.61-67. Center Line, Michigan.
- 12. Kiel, D. F. and Ruble, W. L. "Use of the Core Routine to Calculate Multiple Regressions (Least Squares Fits to Arbitrary Functions) on the CDC 3600." Agricultural Experiment Station, M.S.U. AES Program Description 4.
- 13. Perry, Charles C. (1955) * The Strain Gage Primer.*

 McGraw Hill. New York.
- 14. Proceedings of the First International Rheological Congress. (1948)
- 15. Rayleigh, (1918) * Notes on the Theory of Lubrication.*

 Phil. Mag. Vol.35, pp.1-12.
- 16. S. Oka, (1960) * Rheology: Theory and Applications * (ed. F. R. Eirich) Academic Press. Vol.3.
- 17. Streeter, V. L. (1951) " Fluid Mechanics " McGraw Hill, New York.
- 18. Van Wazer, J. R., Lyons, J. W., Kim, K. Y. and Colwell, R. E. (1963) "Viscosity and Flow Measurement "Interscience Publishers, New York.

ROOM was vinch

TAY 20 68.

ROCH USE OFFICE

